

Interplay between GAD method and conjugate directions to locate transition states

Josep Maria Bofill^{a,b}, Jordi Ribas-Ariño^{c,b}, Rosendo Valero^{c,b}, Guillermo Albareda^{d,b}, Ibério de P.R. Moreira^{c,b}, and Wolfgang Quapp^e

^aDepartament de Química Inorgànica i Orgànica, Universitat de Barcelona, Spain; ^bInstitut de Química Teòrica i Computacional, Universitat de Barcelona, Spain; ^cDepartament de Ciència de Materials i Química Física, Universitat de Barcelona, Spain; ^dMax Planck Institute for the Structure and Dynamics of Matter, Hamburg, Germany; ^eMathematisches Institut, Universität Leipzig, Germany.



ABSTRACT

An algorithm to locate transition states on a Potential Energy Surface (PES) is proposed and described. The technique is based on the Gentlest Ascent Dynamics (GAD) method where the gradient of the PES is projected into a given direction and also perpendicular to it. In the proposed method, named GAD-CD, the projection is not only applied to the gradient but also to the Hessian matrix. Then the resulting Hessian matrix is then block diagonal. The direction is updated according to the gentlest ascent dynamics method. Furthermore, to ensure stability and to avoid high computational cost, a trust region technique is incorporated and the Hessian matrix is updated at each iteration. The performance of the algorithm in comparison with the standard ascent dynamics is discussed for a simple two dimensional model PES. Its efficiency for describing reaction mechanisms involving small and medium size molecular systems is demonstrated for five molecular systems of interest.

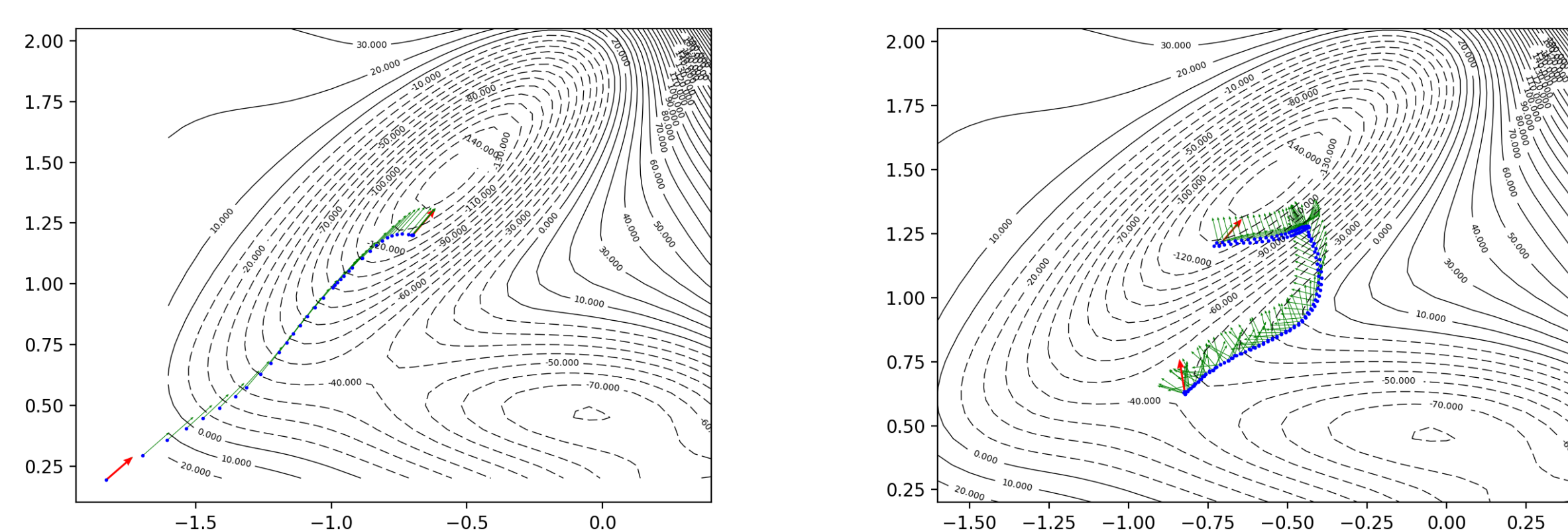
GAD vs GAD-CD

GAD

$$\frac{dx}{dt} = -[\mathbf{I} - 2\mathbf{v}\mathbf{v}^T]\mathbf{g}(\mathbf{x})$$
$$\frac{dv}{dt} = -[\mathbf{I} - \mathbf{v}\mathbf{v}^T]\mathbf{H}(\mathbf{x})\mathbf{v}$$

GAD-CD

$$\mathbf{a} = -(\mathbf{M}_0 + \lambda\mathbf{I})^{-1}\mathbf{h}_0,$$
$$\mathbf{a}^T\mathbf{a} - r^2 = 0; \quad \Delta\mathbf{x}_0 = \mathbf{V}\mathbf{a}$$
$$\mathbf{v}'_1 = s[\mathbf{v}_1 - m(\mathbf{I} - \mathbf{v}_1\mathbf{v}_1^T)\mathbf{H}_0\mathbf{v}_1]$$



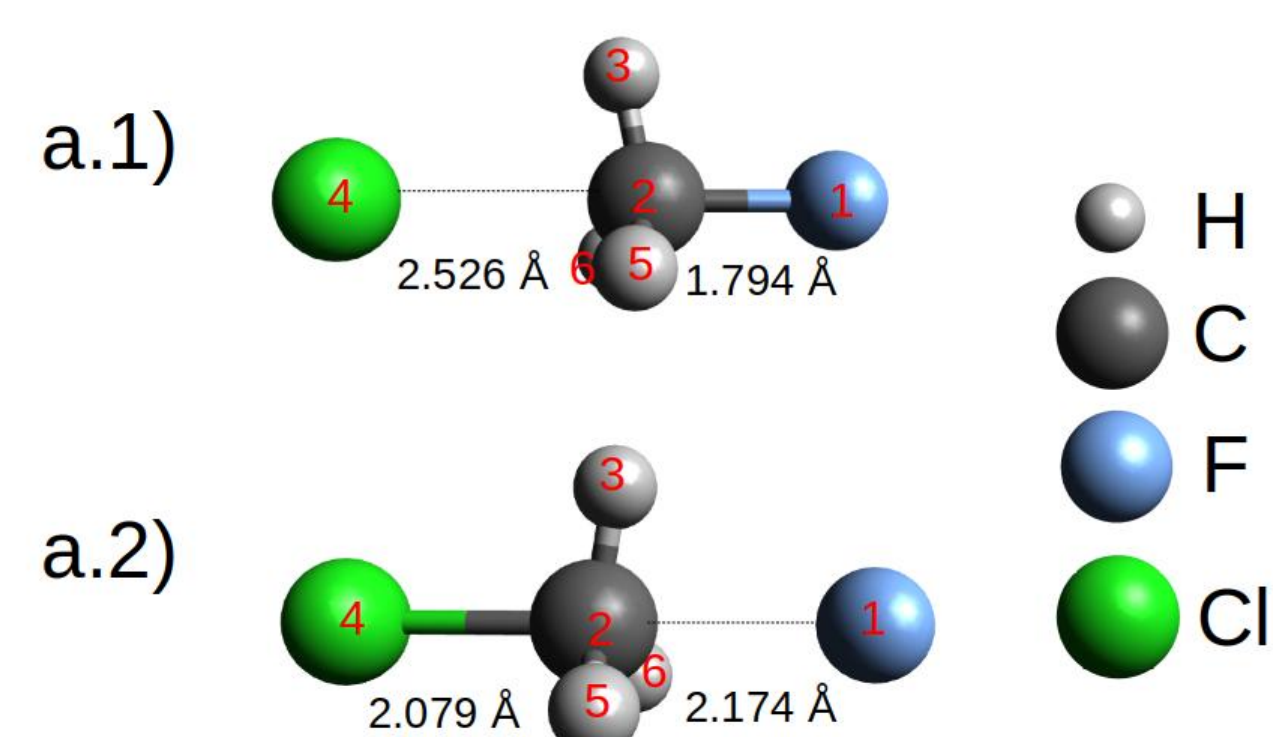
Behavior of GAD and GAD-CD methods on the two-dimensional Müller-Brown PES. The two curves are depicted in blue color. The set of arrows showing the evolution of the control \mathbf{v} -vector is depicted in green color. The two red arrows are the initial and final control vectors. In both methods the starting point of the curve is $(-0.7, 1.2)$. The initial control vector, \mathbf{v}_1 , corresponds to the eigenvector with lowest eigenvalue of the Hessian matrix evaluated in this point. The achieved TS by the GAD-CD method is that located at the point $(-0.822, 0.624)$. The GAD method does not converge to a TS.

THE GAD-CD ALGORITHM

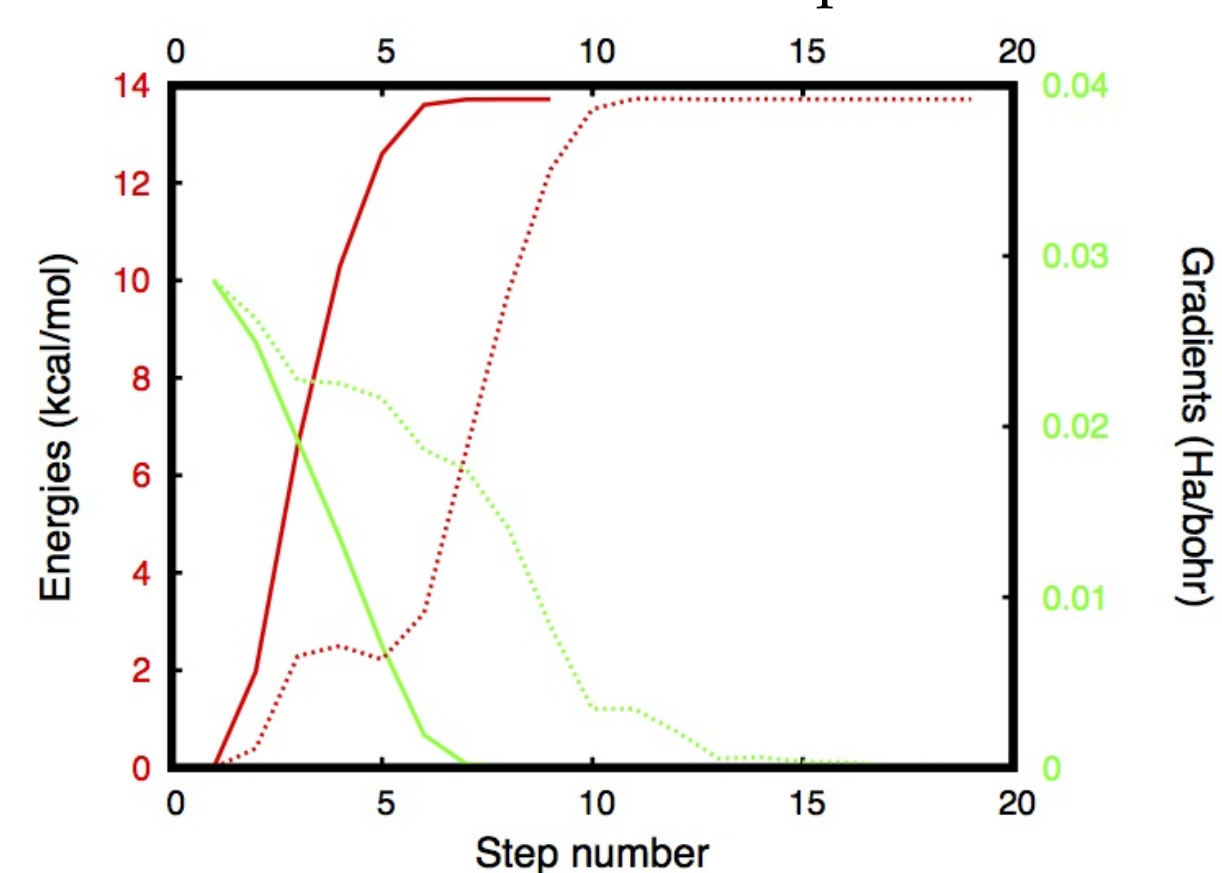
- Initialization:** (a) Choose a guess \mathbf{x}_0 and an initial trust radius r_0 . (b) Calculate the potential energy, V_0 , the gradient vector, \mathbf{g}_0 , and the Hessian matrix, \mathbf{H}_0 . (c) Select the normalized $\mathbf{v}_1^{(0)}$ -vector, usually an eigenvector of the \mathbf{H}_0 matrix. (d) Set $i = 0$.
- Hessian and gradient transformation:** (a) Compute the element $\mathbf{v}_1^{(i)T}\mathbf{H}_i\mathbf{v}_1^{(i)}$. (b) Evaluate the vector $\mathbf{w}^{(i)} = \mathbf{t}^{(i)} - \|\mathbf{t}^{(i)}\|\mathbf{e}_1$ where $\mathbf{t}^{(i)} = \mathbf{H}_i\mathbf{v}_1^{(i)}$, and hence calculate $\mathbf{Q}^{(i)}$. Obtain the $\mathbf{V}_{N-1}^{(i)}$ matrix from $\mathbf{Q}^{(i)}$ by taking the last $N-1$ columns. (c) Calculate $\mathbf{V}_{N-1}^{(i)T}\mathbf{H}_i\mathbf{V}_{N-1}^{(i)}$ and $\mathbf{h}_i = [-\mathbf{v}_1^{(i)}|\mathbf{V}_{N-1}^{(i)}]^T\mathbf{g}_i$. (d) Build the \mathbf{M}_i -matrix taking into account that $\mathbf{v}_1^{(i)T}\mathbf{H}_i\mathbf{v}_1^{(i)}$ should be multiplied by -1 , $\mathbf{v}_1^{(i)T}\mathbf{H}_i\mathbf{v}_1^{(i)} \rightarrow -\mathbf{v}_1^{(i)T}\mathbf{H}_i\mathbf{v}_1^{(i)}$.
- Solution of the restricted step problem:** (a) Compute the Newton step, $\mathbf{a}^{(i)} = -\mathbf{M}_i^{-1}\mathbf{h}_i$. If $\mathbf{a}^{(i)T}\mathbf{a}^{(i)} \leq r_i^2$, $\mathbf{v}_1^{(i)T}\mathbf{H}_i\mathbf{v}_1^{(i)} < 0$ and $\det(\mathbf{V}_{N-1}^{(i)T}\mathbf{H}_i\mathbf{V}_{N-1}^{(i)}) > 0$ then the problem is solved. If $\mathbf{a}^{(i)T}\mathbf{a}^{(i)} < r_i^2$ then $r_i = (\mathbf{a}^{(i)T}\mathbf{a}^{(i)})^{1/2}$ is taken as the current trust radius. Compute the predicted energy change $q_{optimal} - V(\mathbf{x}_i) = -1/2\mathbf{h}_i^T\mathbf{M}_i^{-1}\mathbf{h}_i$, otherwise, (b) solve the non-symmetric eigenproblem, take the real triple of lowest $\lambda_1^{(i)} = \lambda^{(i)}$. Compute $\mathbf{a}_1^{(i)}$ and evaluate $q_{optimal} - V(\mathbf{x}_i)$. Set $\mathbf{a}_1^{(i)} = \mathbf{a}^{(i)}$.
- Trust region verification:** (a) Calculate the potential energy at the new point, $V_{new}^{(i)} = V(\mathbf{x}_i + \mathbf{V}^{(i)}\mathbf{a}^{(i)})$ where $\mathbf{V}^{(i)} = [\mathbf{v}_1^{(i)}|\mathbf{V}_{N-1}^{(i)}]$. (b) Evaluate $c_i = (V_{new}^{(i)} - V(\mathbf{x}_i))/(q_{optimal} - V(\mathbf{x}_i))$. (c) If $c_i \leq c_{min}$ or $c_i \geq (2 - c_{min})$ then $r_{i+1} = r_i/c_f$. (d) If $c_i \geq c_{accept}$ and $c_i \leq (2 - c_{accept})$ and $\mathbf{a}^{(i)T}\mathbf{a}^{(i)} < r_i^2$, then a pure Newton step leads to $r_{i+1} = r_i \cdot (c_f)^{1/2}$.
- Acceptation of the current step:** (a) If $c_i < 2$ or $c_i > 2$ compute the new change $\Delta\mathbf{x}_i = \mathbf{V}^{(i)}\mathbf{a}^{(i)}$ at the same point \mathbf{x}_i but using the updated $r_{i+1} \rightarrow r_i$, and go back to 3. Otherwise, (b) check the convergence criteria on $\{|\Delta\mathbf{x}_i|_{\mu}\}_{\mu=1}^N \leq \epsilon_x$ and $\{|\mathbf{g}_i|_{\mu}\}_{\mu=1}^N \leq \epsilon_g$. If they are fulfilled, the process has converged and the point \mathbf{x}_i is the first-order saddle point. Otherwise, (c) make $\mathbf{x}_{i+1} = \mathbf{x}_i + \Delta\mathbf{x}_i$, $V_{new}^{(i)} = V(\mathbf{x}_{i+1})$, and compute $\mathbf{g}(\mathbf{x}_{i+1}) = \mathbf{g}_{i+1}$. Update the \mathbf{v}_1 and set $\mathbf{v}_1^{(i+1)}$ to the new vector. Finally update the approximate Hessian matrix. Set $i = i + 1$ and go back to 2.

PERFORMANCE FOR THE *sn2* REACTION

Reactant transition state geometries.



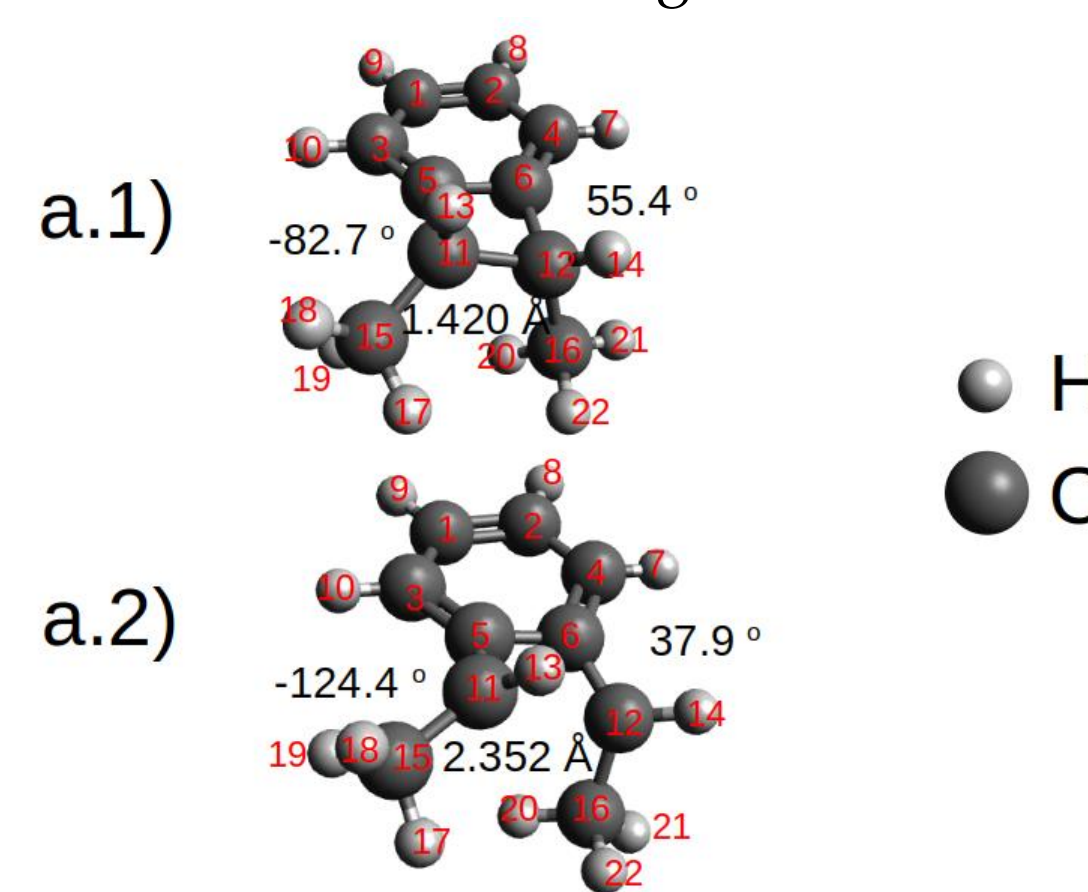
Behavior of location process.



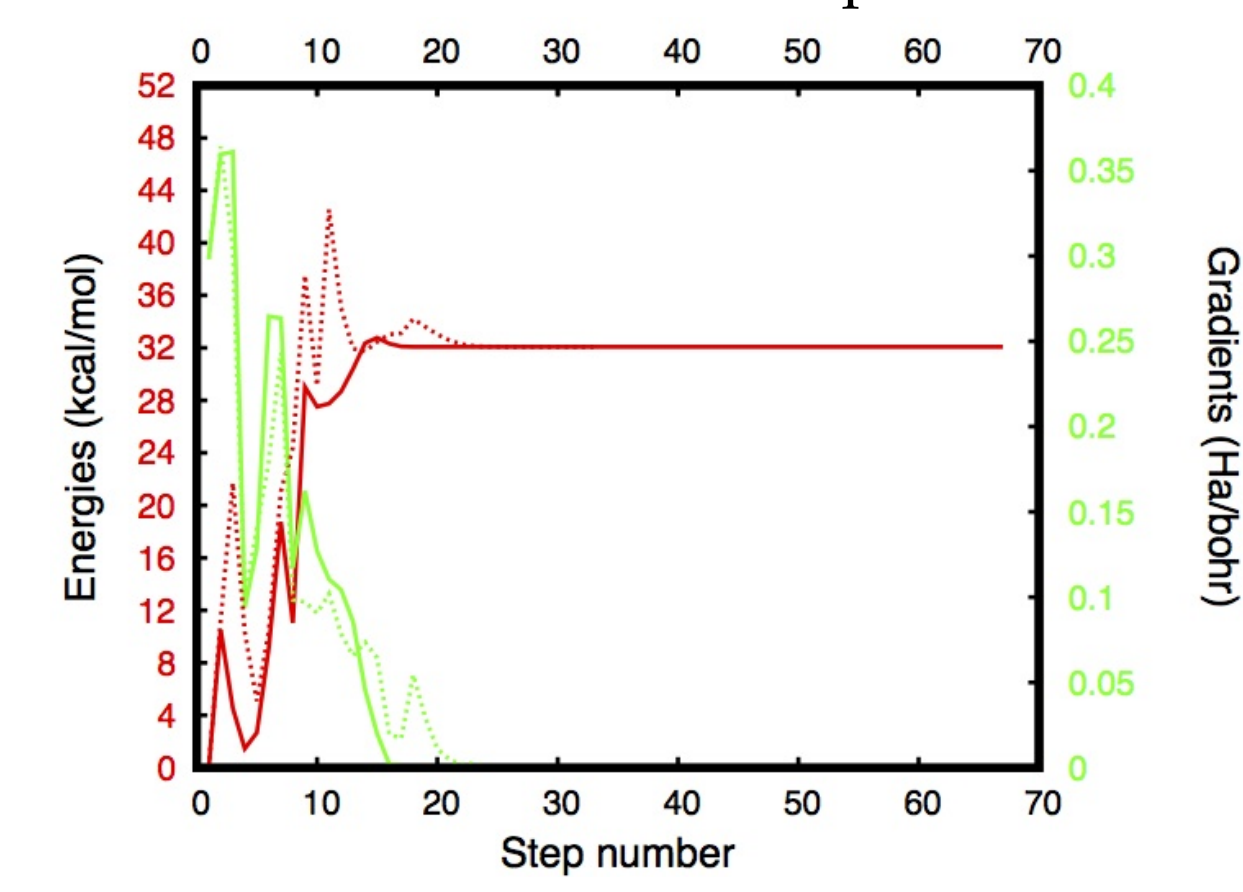
Performance of GAD-CD for the *sn2* reaction, $\text{Cl}^\ominus + \text{CH}_3\text{F} \rightarrow \text{ClCH}_3 + \text{F}^\ominus$. The distances between F and C and between C and Cl, are shown for the initial structure (a.1) and the converged TS (a.2). The evolution of the energy (in Kcal/mol) and maximum component in absolute value of the gradient (in Ha/bohr), $\max\{|\mathbf{g}_\mu|\}_{\mu=1}^N$, as a function of the step number during the TS search for **sn2.2.1** (solid lines) and for **sn2.2.2** (dashed lines) are shown in (b).

PERFORMANCE FOR THE *bc* REACTION

Reactant transition state geometries.



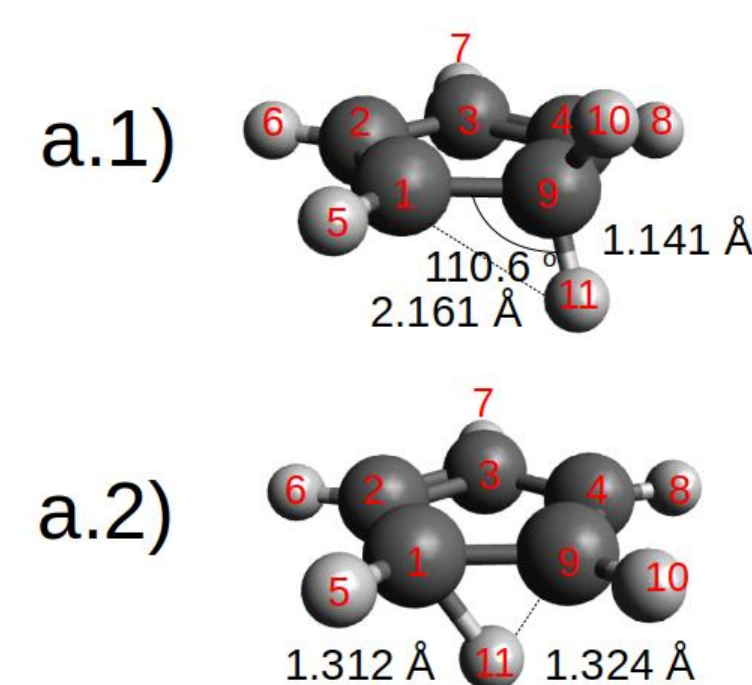
Behavior of location process.



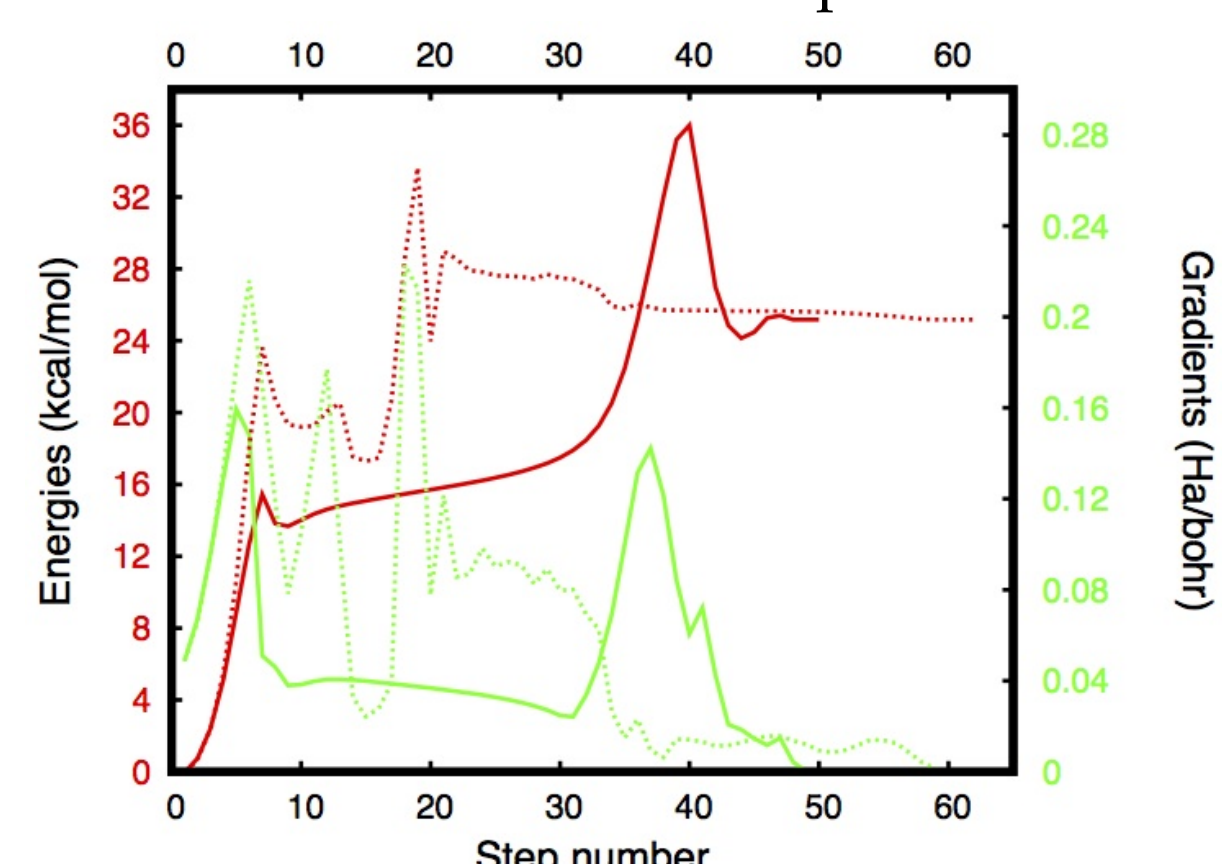
GAD-CD performance for the *bc* reaction, *cis*-1,2-dimethyl-benzocyclobutene \rightarrow *E,Z*-diene. The distance between C11 and C12, the dihedral between C3, C5, C11, and C15, and that between C4, C6, C12, and C16, are shown for the initial structure (a.1) and the converged TS (a.2). The evolution of the energy and maximum component in absolute value of the gradient, $\max\{|\mathbf{g}_\mu|\}_{\mu=1}^N$, as a function of the step number during the TS search for **bcb.3.3** (solid lines) and for **bcb.3.6** (dashed lines) are shown in (b).

PERFORMANCE FOR THE *sig* REACTION

Reactant transition state geometries.



Behavior of location process.



Performance of GAD-CD for the *sig* reaction, [1,5]-H shift in 1,3-cyclopentadiene. The distances between C9 and H11 and between C1 and H11 are shown for the initial structure (a.1) and the converged TS (a.2). The evolution of the energy and maximum component in absolute value of the gradient, $\max\{|\mathbf{g}_\mu|\}_{\mu=1}^N$, as a function of the step number during the TS search for **sig.3.1** (solid lines) and for **sig.3.4** (dashed lines) are shown in (b).

ACKNOWLEDGEMENTS

The authors thank to the financial support from the Spanish Ministerio de Economía y Competitividad, Projects No. CTQ2016-76423-P, CTQ2017-87773-P and Spanish Structures of Excellence María de Maeztu program through grant MDM-2017-0767 and Generalitat de Catalunya, Project No. 2017 SGR 348. G.A. acknowledges also financial support from the European Union's Horizon 2020 research and innovation programme under the Marie Skłodowska-Curie grant agreement No 752822.

REFERENCES

- [1] W. E, X. Zhou, Nonlinearity, 24, 1831 (2011); [2] J. M. Bofill, W. Quapp, M. Caballero, Chem. Phys. Lett., 583, 203 (2013); [3] W. Quapp, J. M. Bofill, Theor. Chem. Acc., 133, 1510 (2014); [4] G. Albareda, JM Bofill, I de PR Moreira, W Quapp, J Rubio-Martínez, Theo. Chem. Acc. 137, 73 (2018); [5] G. Albareda et al., J. Chem. Phys. Lett. 6, 1529 (2015); [6] J. M. Bofill, J. Ribas-Ariño, R. Valero, G. Albareda, I. de P.R. Moreira, W. Quapp, Submitted to JCTC (2019);